

## ON THE GLOBAL VARIATIONS OF TERRESTRIAL HEAT-FLOW\*

W. H. K. LEE

*National Center for Earthquake Research, U.S. Geological Survey, Menlo Park, California 94025, U.S.A.*

Received 10 November 1969

Over 3500 measurements of surface heat-flux have been catalogued and analyzed to study the large-scale variations of terrestrial heat-flow. It was found that heat-flow values are correlated with major geologic provinces: higher averages and scattered values in active tectonic regions, and lower averages and more uniform

values in stable areas. Analyzing the data in the light of new global tectonics shows that the variations of heat-flow are consistent with the hypotheses of sea-floor spreading and plate tectonics. The observed heat-flow across the mid-oceanic ridges can be accounted for by a simple model of a spreading sea floor.

### 1. Introduction

In this paper, large-scale variations of terrestrial heat-flow over the Earth are examined. The basic data used here are derived from measurements of conductive heat-flux across the Earth's surface. Techniques of measuring heat-flow are well known (BECK, 1965; LANGSETH, 1965), and they will not be described here. The present paper is divided into four parts:

- (1) a brief review of the available heat-flow data;
- (2) a brief summary of the results of data analysis;
- (3) an examination of the data to see whether or not they are consistent with the hypotheses of sea-floor spreading and plate tectonics;
- (4) a construction of a simple thermal model based on sea-floor spreading to account for the heat-flow observed across the mid-oceanic ridges.

Because the available time did not permit a detailed report in the Symposium, the present paper (which follows closely the oral presentation) is of necessity brief and should be regarded as a preliminary report. Furthermore, no attempt has been made to review the available literature, and results of data analysis discussed here are mainly my own work which is still in progress. A more detailed study will be published later elsewhere.

### 2. Heat-flow data

Reliable heat-flow measurements on land were first published by BULLARD (1939) and BENFIELD (1939). The first measurements at sea were published by REVELLE and MAXWELL (1952) using what is now called the Bullard-type probe. However, most data have been gathered only since 1963 when the techniques of measuring heat-flow became well developed and many geophysicists became interested in heat-flow studies. At present, about 4000 heat-flow measurements have been made through the industrious efforts of many workers all over the world. They deserve great credit, for without their measurements the present paper would not be possible.

Because there is some delay in publication, only about 3000 measurements have been published. As of August 1969, the author has collected 3564 measurements of which about 500 are as yet to be published. Since 1968, over 600 heat-flow measurements have been made annually, and it is hoped that such a high rate of output will be maintained in the future.

A convenient way to summarize the presently available heat-flow data is by means of maps containing  $5^\circ \times 5^\circ$  data numbers and averages, as shown in figs. 1 and 2. Heat-flow data were catalogued following a procedure similar to that of LEE and UYEDA (1965). Nearby and repeated measurements were grouped together. Data were graded rather subjectively in a five-

\* Publication authorized by the Director of the U.S. Geological Survey.

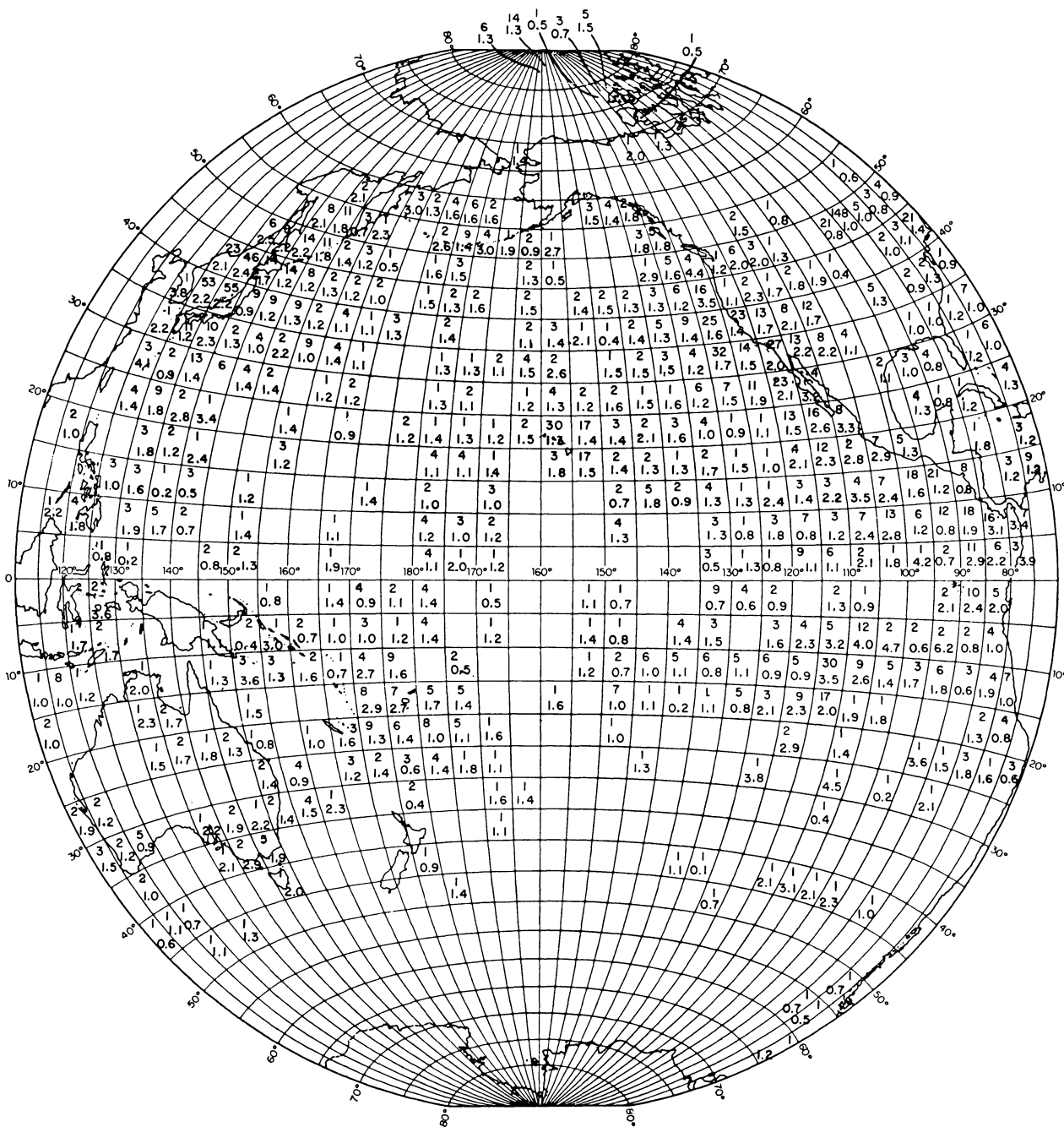


Fig. 1. Heat-flow data in  $5^{\circ} \times 5^{\circ}$  grid. In each grid element, the upper value is the number of data, and the lower value is the arithmetic mean with quality weighting in  $\mu\text{cal}/\text{cm}^2$ .

point scale which corresponds to the overall error estimates ( $\epsilon$ ) as shown in table 1. In estimating the assigned weight, I had considered the site conditions and the manner in which the temperature gradient and the

thermal conductivity were measured. Error estimates by the original authors were also taken into account if they were available. A total of 3564 measurements were catalogued, some of which were grouped together to

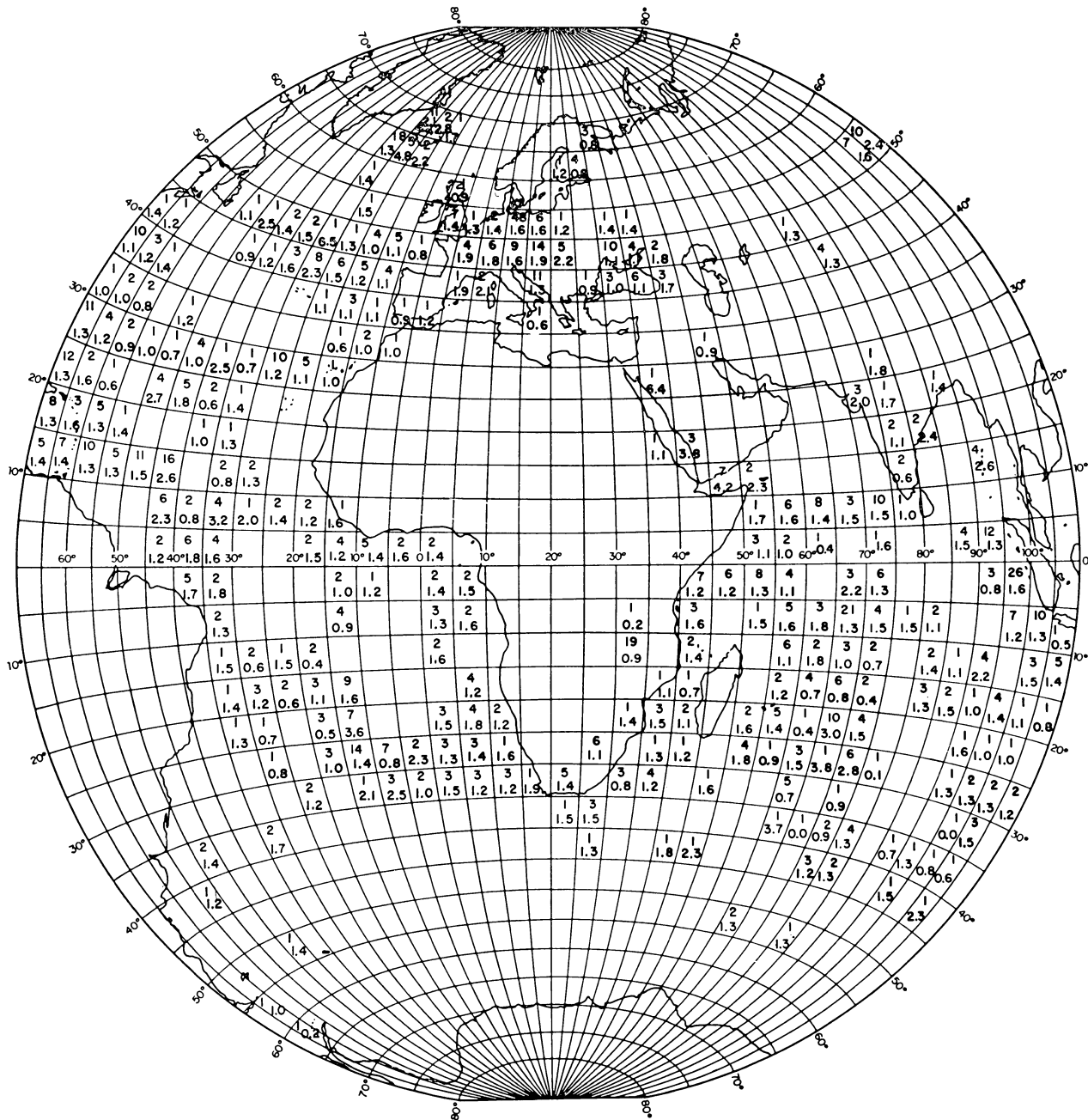


Fig. 2. Heat-flow data in  $5^{\circ} \times 5^{\circ}$  grid. In each grid element, the upper value is the number of data, and the lower value is the arithmetic mean with quality weighting in  $\mu\text{cal}/\text{cm}^2$ .

give a total of 3231 heat-flow data. After rejecting 104 heat-flow data as unreliable, 3127 data were analysed.

The distribution of heat-flow data is extremely uneven geographically as can be seen from figs. 1 and 2. Because heat-flow measurements are more easily made

at sea, oceanic data outnumber continental measurements by a ratio of about 4 to 1. Large data gaps exist in Asia, Africa, South America, Antarctica, and high-latitude oceanic regions where additional measurements should be carried out.

TABLE 1  
Grading scale for heat-flow data

Classification	Assigned weight	Error estimates
Excellent	5	$\epsilon \leq 10\%$
Good	4	$10\% < \epsilon \leq 20\%$
Fair	3	$20\% < \epsilon \leq 30\%$
Poor	2	$30\% < \epsilon \leq 40\%$
Very poor	1	$40\% < \epsilon \leq 50\%$
Unreliable	0	$\epsilon > 50\%$

3. Data analysis

The present data analysis differs in one important aspect from all other analyses (e.g. LEE and UYEDA, 1965; VON HERZEN and LEE, 1969; LANGSETH and VON HERZEN, 1970), namely that the heat-flow data are weighted according to their quality in a five-point scale (table 1). This weighting permits a less severe cut-off in rejecting poor-quality data and takes into account the fact that heat-flow measurements do not give uniform-quality data. The  $5^\circ \times 5^\circ$  averages shown in figs. 1 and 2 are obtained with such weighting, and quality weighting has been employed throughout all subsequent data analysis.

TABLE 2

Statistics of heat-flow values for various geographical divisions  
 N — number of data  
 $\bar{q}$  — arithmetic mean with quality weighting in  $\mu\text{cal}/\text{cm}^2\text{s}$   
 S.D. — standard deviation from the mean with quality weighting in  $\mu\text{cal}/\text{cm}^2\text{s}$

Area	Individual values			Equal-area grid averages*		
	N	$\bar{q}$	S.D.	N	$\bar{q}$	S.D.
World	3127	1.63	1.07	673	1.47	0.74
All continents	597	1.45	0.57	95	1.46	0.46
All oceans	2530	1.67	1.15	591	1.47	0.78
Atlantic Ocean	436	1.47	1.14	126	1.34	0.57
Indian Ocean	358	1.36	0.95	108	1.32	0.52
Pacific Ocean	1308	1.70	1.24	310	1.50	0.84

\*  $9 \times 10^4$  square nautical miles per grid element, or  $5^\circ \times 5^\circ$  at the equator

Statistics of heat-flow values for various geographical divisions of the Earth are summarized in table 2. These statistics are based on individual values as well as equal-area grid averages. Because of uneven geographical distribution of heat-flow data, statistics based on

individual values must be interpreted with caution. In order to compensate for this sampling bias, statistics weighted according to surface area were introduced by LEE and UYEDA (1965). Since grid elements formed by equally spaced intervals of latitude and longitude have unequal surface area, geographical grid averages do not give an unbiased sample. To avoid this difficulty, averages for grid elements of equal area ( $9 \times 10^4$  square nautical miles, or  $5^\circ \times 5^\circ$  at the equator) were computed and statistically analyzed.

Table 2 reveals that the arithmetic mean and standard deviation for grid averages are less than that for the original data. The likely interpretations are that the geographic density of measurements is greater in regions of high heat-flow, and that some local variability is removed by grid averaging. Histograms of heat-flow grid averages for the world, continents, and oceans are shown in fig. 3. However, detailed comparison between

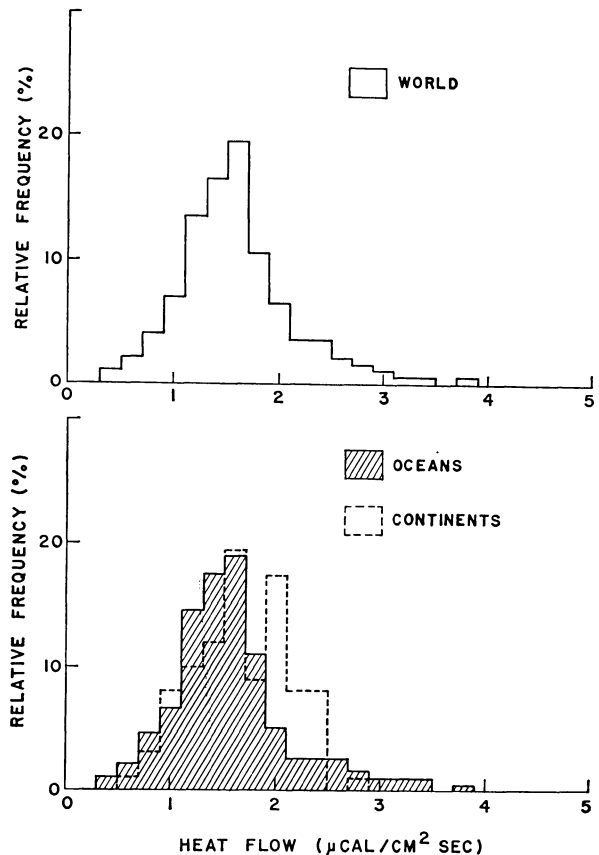


Fig. 3. Histograms of equal-area grid averages of heat-flow for the world, continents and oceans.

oceanic and continental histograms is as yet premature because of the limited data coverage on land. The arithmetic mean is  $1.47 \mu\text{cal}/\text{cm}^2\text{s}$  for oceanic heat-flow grid averages and is  $1.46 \mu\text{cal}/\text{cm}^2\text{s}$  for continents. The difference is insignificant and confirms the equality of heat flux through continental and oceanic regions.

Statistics of heat-flow values for various tectonic regions of the Earth are summarized in table 3. Corresponding histograms are shown in figs. 4 and 5. As pointed out by LEE and UYEDA (1965), heat-flow values seem to correlate with major geologic provinces. Results of the present analysis further confirm such correlation. Precambrian shields are characterized by low and rather uniform values, whereas Mesozoic–Cenozoic orogenic areas have high and more scattered values. A similar pattern exists between ocean basins and mid-oceanic ridges. Because different geologic provinces are in various stages of tectonic development, such a correlation is to be expected.

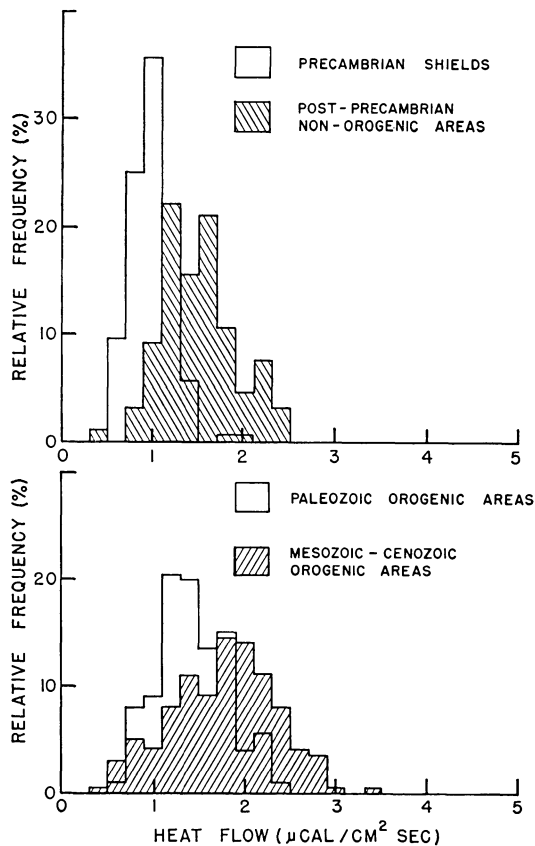


Fig. 4. Heat-flow histograms for various tectonic provinces on land.

TABLE 3

Statistics of heat-flow values for various tectonics regions  
 $N$  – number of data  
 $\bar{q}$  – arithmetic mean with quality weighting in  $\mu\text{cal}/\text{cm}^2\text{s}$   
 S.D. – standard deviation from the mean with quality weighting in  $\mu\text{cal}/\text{cm}^2\text{s}$

Tectonic region	$N$	$\bar{q}$	S.D.
Precambrian shields	214	0.98	0.24
Post-Precambrian non-orogenic areas	96	1.49	0.41
Palaeozoic orogenic areas	88	1.43	0.40
Mesozoic–Cenozoic orogenic areas	159	1.76	0.58
Ocean basins	683	1.27	0.53
Mid-oceanic ridges	1065	1.90	1.48
Ocean trenches	78	1.16	0.70
Continental margins	642	1.80	0.93

Despite a threefold increase in heat-flow data, results of the present data analysis agree rather well with those found by LEE and UYEDA (1965). The best estimate of the mean heat-flow of the Earth based on a spherical harmonic analysis is

$$\hat{q} = 1.47 \pm 0.08 \mu\text{cal}/\text{cm}^2\text{s} \quad (1)$$

at 95% confidence level which agrees well with the previous estimate of  $1.5 \pm 10\% \mu\text{cal}/\text{cm}^2\text{s}$  by LEE (1963).

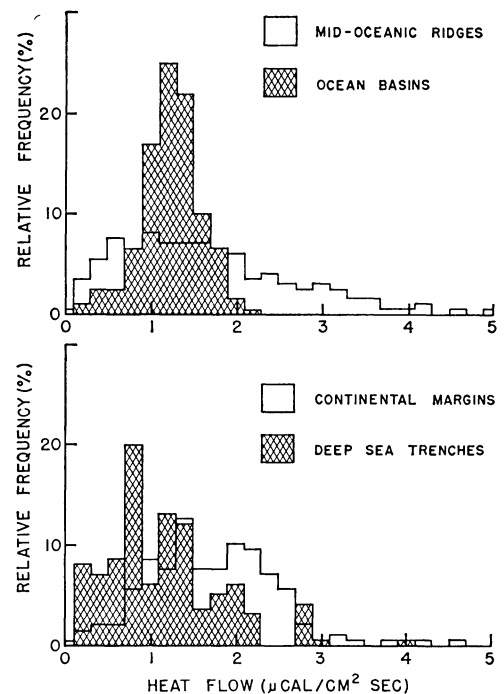


Fig. 5. Heat-flow histograms for various tectonic provinces at sea.

#### 4. Heat-flow and the new global tectonics

In the last few years, new concepts of global tectonics have emerged. The hypothesis of sea-floor spreading by HESS (1962) has been demonstrated by Vine, Heirtzler and others in the magnetic patterns of the ocean floor. The corollary hypothesis of transform faulting by WILSON (1965) has been confirmed by the work of Sykes and his associates. The term "new global tectonics" as used by ISACKS *et al.* (1968) refers to these new concepts and their consequent tectonic implications. In brief, the more rigid lithosphere is believed to be capable of large horizontal movements, new crust is generated at the ridge crest, spreads away from it, and eventually descends down beneath the deep sea trench.

Various geological and geophysical data suggest that the movements of the lithosphere can be accounted for by rotations of large rigid plates (MORGAN, 1968; LE PICHON, 1968). To a first approximation, Le Pichon divided the Earth into six main blocks as shown in

fig. 6. The boundaries are either ridge crests, or trenches, or transform faults. Since each plate moves more or less as a single unit, active tectonic processes occur mainly along its edges as demonstrated by the distribution of earthquake foci (ISACKS *et al.*, 1968).

As tectonic processes involve changes of energy, one may expect that the heat-flow will fluctuate more near the edge of each plate than at its interior. This may be tested by plotting the heat-flow standard deviation in  $5^\circ \times 5^\circ$  squares as is also shown in fig. 6. Because the standard deviation in each  $5^\circ \times 5^\circ$  square can be computed only if there are two or more values in it, there are less data to work with than the averages in figs. 1 and 2. For the purpose of discussion, variation of heat-flow is considered low if the standard deviation is less than  $0.5 \mu\text{cal}/\text{cm}^2\text{s}$ . Examination of fig. 6 shows that the heat-flow data are generally consistent with plate tectonics: large heat-flow variations occurring approximately along the edges of the tectonic plates and low variations at their interior regions. There are, however, some exceptions which may be caused by insufficient

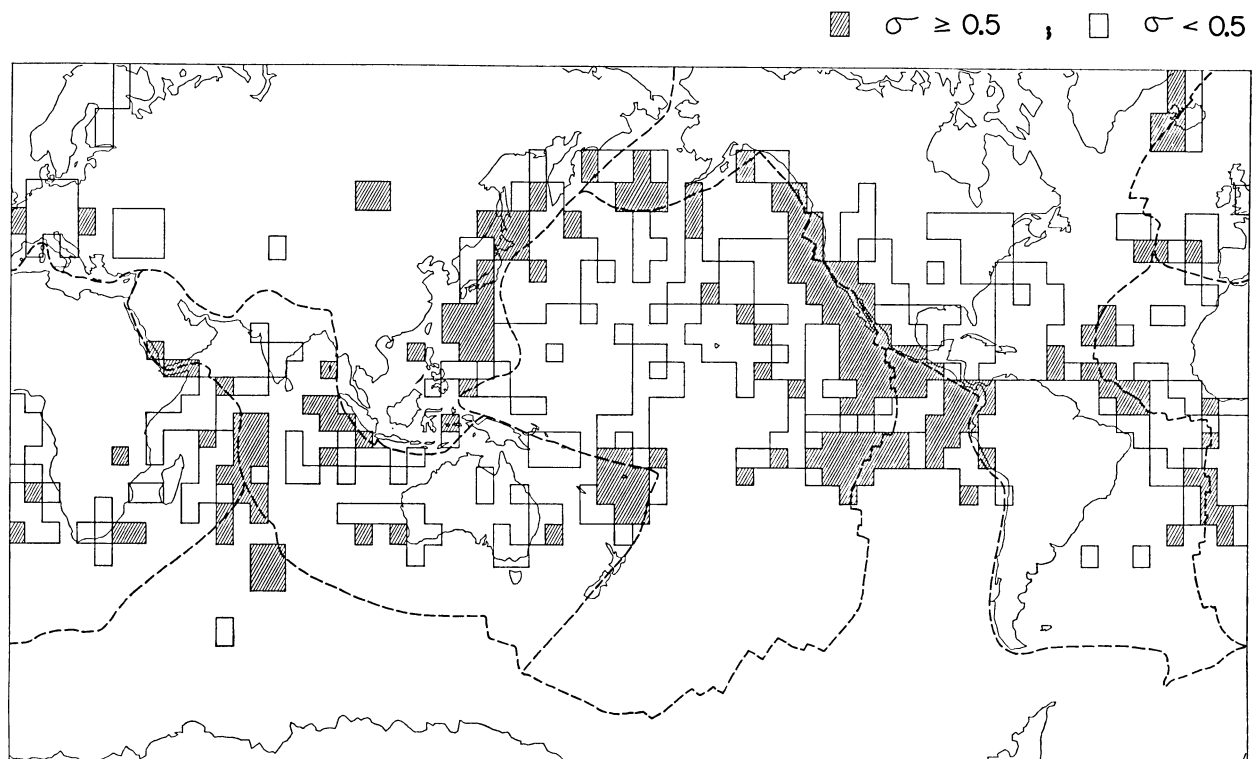


Fig. 6. Heat-flow standard deviations ( $\sigma$ ) in  $5^\circ \times 5^\circ$  grid. Data are available only in enclosed rectangular-shaped areas. If  $\sigma \geq 0.5 \mu\text{cal}/\text{cm}^2\text{s}$ , the enclosed areas are shaded. Heavy dashed lines are boundaries of the six major tectonic blocks according to LE PICHON (1968).

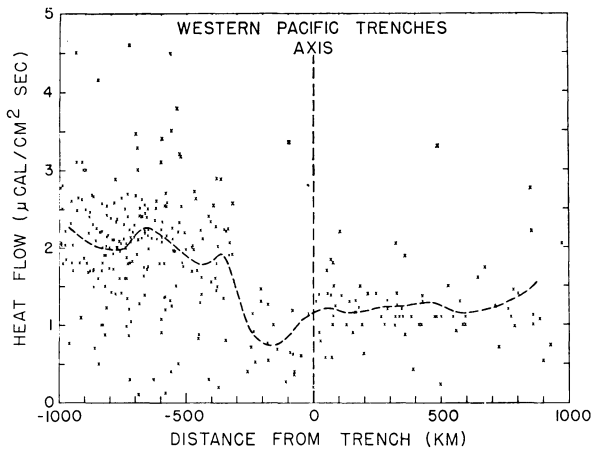


Fig. 7. Heat-flow versus the distance from the trench axis for the western Pacific Ocean. Distance is positive towards the oceans and negative towards the continents. The dashed curve is based on the arithmetic average with quality weighting of values in each 100 km distance interval.

numbers of measurements and/or local conditions.

A great deal of interest has been focused on the island-arc trench regions where the lithospheric plates descend. A plot of heat-flow versus the distance from the trench axis for the western Pacific Ocean is shown in fig. 7. Distance is positive towards the oceans and

negative towards the continents. The dashed curve is based on the arithmetic average with quality weighting of values in each 100 km distance interval. Average heat-flow is about  $1.3 \mu\text{cal}/\text{cm}^2\text{s}$  in the ocean basin but dips below  $1 \mu\text{cal}/\text{cm}^2\text{s}$  at about 200 km behind the trench axis and rises rapidly to  $2 \mu\text{cal}/\text{cm}^2\text{s}$  in the inland seas. This pattern of heat-flow is consistent with the idea that the lithospheric plate is descending down below the trench. The high heat-flow in the inland seas may be due to various heating processes near the boundary of the descending plate. D. P. McKenzie and S. Uyeda independently suggested some possible models at the IASPEI/IAGA meetings. This problem had also been studied by MCKENZIE and SCLATER (1968), RALEIGH and LEE (1968), and TURCOTTE and OXBURGH (1968).

Another test of Le Pichon's model of plate tectonics is to plot the heat-flow versus the age of the sea floor. On a sphere, the motion of one block relative to another block corresponds to a rotation about a pole (MORGAN, 1968, p. 1962). The angular velocity or spreading rate is largest near the rotational equator and decreases toward the rotational pole. To compute the age of the sea floor for a given heat-flow station, one needs the distance from the ridge axis and its spreading rate. The

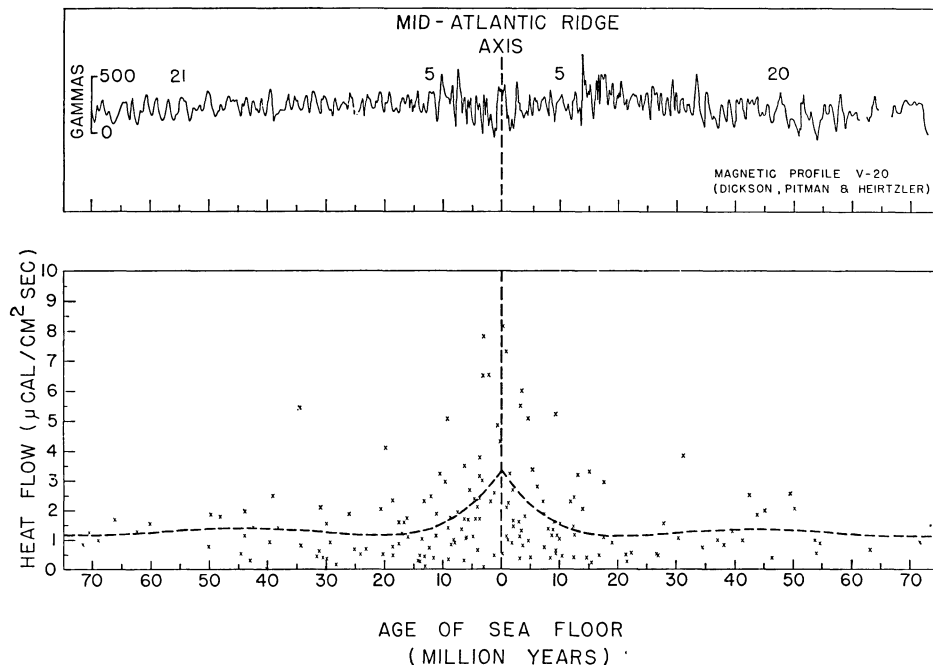


Fig. 8. Heat-flow versus the age of the sea floor for the Mid-Atlantic Ridge. See text for explanation.

spreading rate for every heat-flow station is computed from the pole position and maximum angular velocity of rotation given in table 4, which is taken from LE PICHON (1968). Combining with the corresponding distance from the ridge axis, we obtain the age of the sea floor for every given heat-flow station.

Fig. 8 shows heat-flow versus the age of the sea floor for the Mid-Atlantic Ridge. The dashed curve is a least-squares fit of the data to fifth degree polynomials:

$$q(t) = \sum_{i=0}^5 A_i t^i, \quad (2)$$

where  $q$  is the heat-flow,  $t$  the age of the sea floor, and  $A_i$  the coefficients obtained from the least-squares fit. We have used eq. (2) because the fit does not improve significantly beyond the fifth degree.

The data were actually fitted in three different ways: data from the east side of the Mid-Atlantic Ridge, data from the west side of the Mid-Atlantic Ridge, and combined data without regard to the direction from the Mid-Atlantic Ridge. Since the resulting curves do not differ appreciably, the curve shown in fig. 8 is based on the combined data and is therefore automatically symmetrical with respect to the ridge axis. From fig. 8 one can examine how the data are fitted to a symmetric pattern. For comparison, a magnetic profile taken from DICKSON *et al.* (1968) is shown above. One important feature of fig. 8 is the change in character of both magnetic and heat-flow profiles at about  $10^7$  y. A

TABLE 4  
Data used for computing the age of sea floor; based on LE PICHON (1968) p. 3665

	Rotation-pole position		Maximum angular velocity ( $10^{-7}$ °/y)
	Latitude	Longitude	
Atlantic	69° N	32° W	3.7
North Pacific	53° N	47° W	6.0
South Pacific	68° S	123° E	10.8

corresponding plot for the East Pacific Rise is shown in fig. 9; it is strikingly similar in shape to that for the Mid-Atlantic Ridge.

Before the concept of sea-floor spreading was widely accepted, LEE and UYEDA (1965) had presented figures of heat-flow versus the distance from the ridge axis for the Mid-Atlantic Ridge, East-Pacific Rise, and the Mid-Indian Ocean Ridge. These figures have been used, for example, by MCKENZIE (1967), OXBURGH and TURCOTTE (1968), SLEEP (1969), and TURCOTTE and OXBURGH (1969) as an observed evidence for testing their various thermal models for the mid-oceanic ridges. However, in the light of the new global tectonics, the age of the sea floor is a more fundamental parameter than the distance from the ridge axis because of different spreading rates along the ridge. Consequently, the new plots (figs. 8 and 9) will be more useful for testing such models.

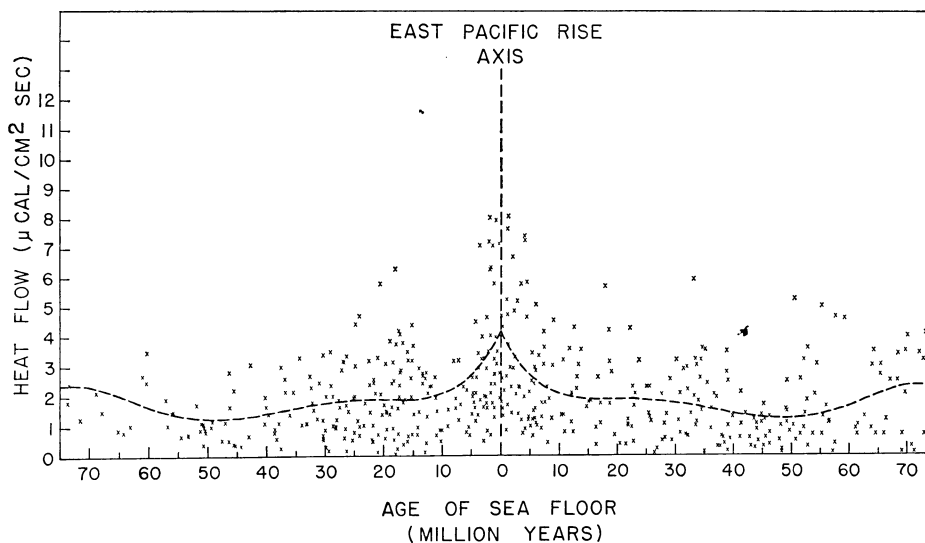


Fig. 9. Heat-flow versus the age of the sea floor for the East Pacific Rise. See text for explanation.

### 5. Thermal model for mid-oceanic ridges

A simple thermal model can be constructed to account for the observed heat-flow profiles in figs. 8 and 9. The model is a semi-infinite slab of thickness  $l$ , moving with a velocity  $v$  in the  $x$  direction, as shown in fig. 1a. The heat equation for this model is

$$\frac{\partial T}{\partial t} = \kappa \left[ \frac{\partial^2 T}{\partial x^2} + \frac{\partial^2 T}{\partial z^2} \right] - v \frac{\partial T}{\partial x}, \quad (3)$$

where  $T$  is the temperature,  $t$  the time, and  $\kappa$  the thermal diffusivity. Boundary conditions for the temperature are denoted by  $T_0$  at  $z = 0$ ,  $T_1$  at  $-z = l$ , and

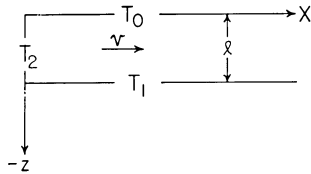


Fig. 10. Thermal model of a semi-infinite slab of thickness  $l$  moving with a velocity  $v$  in the  $x$ -direction.  $T_0$ ,  $T_1$ ,  $T_2$  are the boundary conditions for the temperature.

$T_2$  at  $x = 0$ . Heat production in the slab is ignored as the time scale we are interested in is of the order of tens of millions of years so that the change of radiogenic-heat production is not of prime importance.

MCKENZIE (1967) has obtained an analytic solution for the steady-state equation, i.e. ignoring the  $\partial T/\partial t$  term in eq. (3) and assuming  $T_2 = T_1$ . In this paper, these restrictions were removed, and eq. (3) was solved by a finite difference method using an alternating direction implicit scheme (PEACEMAN and RACHFORD, 1955). The solutions were obtained for a grid of 5 km spacing and a time step depending on the spreading velocity  $v$  (e.g.  $0.25 \times 10^6$  y for  $v = 2$  cm/y). LANGSETH *et al.* (1966) have also studied a similar problem but using an explicit scheme to obtain the solutions.

Fig. 11 illustrates the history of the heat-flow profile for a model where

$$\begin{aligned} T_0 &= 0^\circ\text{C}, & \kappa &= 0.01 \text{ cm}^2/\text{s}, \\ T_1 &= 550^\circ\text{C}, & l &= 50 \text{ km}, \end{aligned}$$

and

$$\begin{aligned} t &= 0-5 \times 10^6 \text{ y}: & v &= 2 \text{ cm/y}, & T_2 &= 550^\circ\text{C}; \\ t &= 5-10 \times 10^6 \text{ y}: & v &= 0, & T_2 &\text{ computed}; \\ t &= 10-15 \times 10^6 \text{ y}: & v &= 2 \text{ cm/y}, & T_2 &= 550^\circ\text{C}; \end{aligned} \quad (4)$$

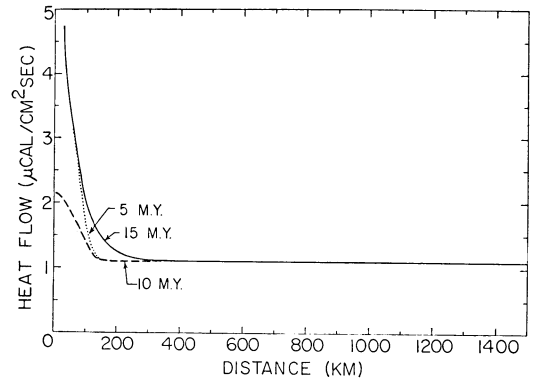


Fig. 11. Heat-flow profiles for an on-off-on spreading model. See text for explanation.

so that it is an on-off-on spreading model. After  $5 \times 10^6$  y of spreading, the heat-flow profile is shown by the dotted curve. If sea-floor spreading stops for another  $5 \times 10^6$  y, the profile at  $10 \times 10^6$  y is the dashed curve. Finally, if the sea floor spreads again for  $5 \times 10^6$  y, the profile at  $15 \times 10^6$  y is the solid curve. It is interesting to note that, except near the ridge crest, the heat-flow profile is rather insensitive to the history of spreading.

For the Mid-Atlantic Ridge, parameters for the model are  $T_0 = 0^\circ\text{C}$ ,  $T_1 = 550^\circ\text{C}$ ,  $\kappa = 0.01 \text{ cm}^2/\text{s}$ ,  $l = 50 \text{ km}$ ,  $T_2 = 800^\circ\text{C}$  at 50 km depth decreasing linearly to  $250^\circ\text{C}$  at the surface and  $v = 2 \text{ cm/y}$ . A history of spreading for  $70 \times 10^6$  y, non-spreading for  $40 \times 10^6$  y and spreading again for  $10 \times 10^6$  y was assumed. The result is shown as the solid curve in fig. 12. The observed profile is dashed and the dotted curve is based on McKenzie's solution for the steady-state equation with  $T_2 = 550^\circ\text{C}$ . The steady-state solution is equivalent to spreading for an infinite period of time.

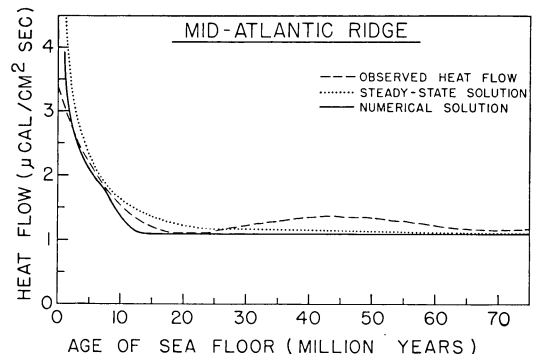


Fig. 12. Heat-flow profiles for the Mid-Atlantic Ridge. See text for explanation.

Either model is consistent with the observed data. It is also interesting to note that the on-off-on spreading model yields a result almost identical to a simple continuous spreading model of just  $10 \times 10^6$  y.

For the East Pacific Rise, the parameters used are  $T_0 = 0^\circ\text{C}$ ,  $T_1 = 750^\circ\text{C}$ ,  $\kappa = 0.01 \text{ cm}^2/\text{s}$ ,  $l = 50 \text{ km}$ ,  $T_2 = 1000^\circ\text{C}$  at 50 km depth decreasing linearly to  $250^\circ\text{C}$  at the surface, and  $v = 4 \text{ cm/y}$  for a spreading of  $10 \times 10^6$  y. Pacific results which correspond to the Atlantic case are shown in fig. 13. Again the models agree quite well with the observed data.

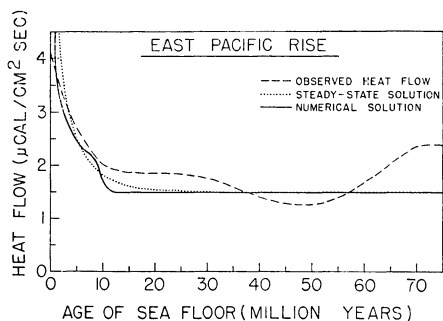


Fig. 13. Heat-flow profiles for the East Pacific Rise. See text for explanation.

Three important results emerge from the above model calculations:

(1) sea floor spreading for  $10 \times 10^6$  y or longer will produce the heat-flow anomaly observed at the mid-oceanic ridges;

(2) a spreading period longer than  $10 \times 10^6$  y yields similar results to a spreading of just  $10 \times 10^6$  y;

(3) effects of non-spreading will be lost after  $10 \times 10^6$  y of spreading.

So the thermal model considered here will not help to resolve the question whether sea-floor spreading is intermittent (EWING and EWING, 1967). However, after the Symposium, L. Sykes kindly pointed out that recent data indicates a continuous spreading of the sea-floor for much of the Atlantic Ocean.

To sum up: analysis of heat-flow data in the light of new global tectonics indicates that the heat-flow data are consistent with the hypotheses of sea-floor spreading and plate tectonics.

#### Acknowledgments

I wish to thank S. Hart, M. Langseth, S. Uyeda,

R. P. von Herzen, and M. Yasui for sending me their unpublished data. I also benefited greatly from the stimulative discussion with L. Sykes and S. Uyeda after the Symposium. The helpful comments on the manuscript by C. B. Raleigh, J. H. Sass and R. P. von Herzen are appreciated.

#### References

- BECK, A. E. (1965), Techniques of measuring heat flow on land. In: W. H. K. Lee, ed., *Terrestrial heat flow* (Am. Geophys. Union, Washington, D.C.) 24.
- BENFIELD, A. E. (1939), Proc. Roy. Soc. London A **173**, 428.
- BULLARD, E. C. (1939), Proc. Roy. Soc. London A **173**, 474.
- DICKSON, G. O., W. C. PITMAN, III and J. R. HEIRTZLER (1968), J. Geophys. Res. **73**, 2087.
- EWING, J. and M. EWING (1967), Science **156**, 1590.
- HESS, H. H. (1962), History of ocean basins. In: A. E. J. Engle, H. L. James and B. L. Leonard, eds., *Petrologic studies* (Geol. Soc. Am., New York) 599.
- ISACKS, B., J. OLIVER and L. R. SYKES (1968), J. Geophys. Res. **73**, 5855.
- LANGSETH, M. G. (1965), Techniques of measuring heat flow through the ocean floor. In: W. H. K. Lee, ed., *Terrestrial heat flow* (Am. Geophys. Union, Washington, D.C.) 58.
- LANGSETH, M. G., X. LE PICHON and M. EWING (1966), J. Geophys. Res. **71**, 5321.
- LANGSETH, M. G. and R. P. VON HERZEN (1970), Heat flow through the floor of the world oceans, in press.
- LEE, W. H. K. (1963), Rev. Geophys. **1**, 449.
- LEE, W. H. K. and S. UYEDA (1965), Review of heat flow data. In: W. H. K. Lee, ed., *Terrestrial heat flow* (Am. Geophys. Union, Washington, D.C.) 87.
- LE PICHON, X. (1968), J. Geophys. Res. **73**, 3661.
- McKENZIE, D. P. (1967), J. Geophys. Res. **72**, 6261.
- McKENZIE, D. P. and J. G. SCLATER (1968), J. Geophys. Res. **73**, 3173.
- MORGAN, W. J. (1968), J. Geophys. Res. **73**, 1959.
- OXBURGH, E. R. and D. L. TURCOTTE (1968), J. Geophys. Res. **73**, 2643.
- PEACEMAN, D. W. and H. H. RACHFORD (1955), J. Soc. Ind. Appl. Math. **3**, 28.
- RALEIGH, C. B. and W. H. K. LEE (1968), Sea-floor spreading and island-arc tectonics. In: *Proc. Conf. on Andesite, Eugene, Ore., 1968*, 99.
- REVELLE, R. and A. E. MAXWELL (1952), Nature **170**, 199.
- SLEEP, N. H. (1969), J. Geophys. Res. **74**, 542.
- TURCOTTE, D. L. and E. R. OXBURGH (1968), Phys. Earth Planet. Interiors **1**, 381.
- TURCOTTE, D. L. and E. R. OXBURGH (1969), J. Geophys. Res. **74**, 1458.
- VON HERZEN, R. P. and W. H. K. LEE (1969), Heat flow in oceanic regions. In: *The Earth's crust and upper mantle*, Geophys. Monograph **13** (Am. Geophys. Union, Washington, D.C.) 88.
- WILSON, J. T. (1965), Nature **207**, 343.